PHYSICAL REVIEW D **76,** 091103(R) (2007)

Measurements of time-dependent CP violation in $B^0 \to \omega K_S^0$, $f_0(980)K_S^0$, $K_S^0\pi^0$ and $K^+K^-K_S^0$ decays

Y. Chao,[24] K.-F. Chen,[24] H. Miyake,[30] O. Tajima,[8] K. Trabelsi,[8] K. Abe,[8] K. Abe,[40] I. Adachi,[8] H. Aihara,[42] D. Anipko,[1] A. M. Bakich,[38] E. Barberio,[19] U. Bitenc,[12] I. Bizjak,[12] S. Blyth,[22] A. Bondar,[1] M. Bračko,[8,12,18] T. E. Browder,[7] M.-C. Chang,[4] P. Chang,[24] A. Chen,[22] W. T. Chen,[22] B. G. Cheon,[6] R. Chistov,[11] Y. Choi,[37] Y. K. Choi,[37] S. Cole,[38] J. Dalseno,[19] M. Danilov,[11] M. Dash,[46] J. Dragic,[8] A. Drutskoy,[3] S. Eidelman,[1] S. Fratina,[12] N. Gabyshev,[1] B. Golob,[12,17] H. Ha,[14] J. Haba,[8] K. Hara,[20] T. Hara,[30] N. C. Hastings,[42] H. Hayashii,[21] M. Hazumi,[8] D. Heffernan,[30] T. Higuchi,[8] T. Hokuue,[20] Y. Hoshi,[40] W.-S. Hou,[24] Y. B. Hsiung,[24] T. Iijima,[20] K. Ikado,[20] K. Inami,[20] A. Ishikawa,[42] H. Ishino,[43] R. Itoh,[8] M. Iwasaki,[42] Y. Iwasaki,[8] H. Kaji,[20] J. H. Kang,[47] P. Kapusta,[25] H. Kawai,[2] T. Kawasaki,[27] H. J. Kim,[15] H. O. Kim,[37] Y. J. Kim,[5] K. Kinoshita,[3] S. Korpar,[18,12] P. Križan,[12,17] P. Krokovny,[8] R. Kulasiri,[3] R. Kumar,[31] C. C. Kuo,[22] A. Kuzmin,[1] Y.-J. Kwon,[47] M. J. Lee,[35] T. Lesiak,[25] A. Limosani,[8] S.-W. Lin,[24] D. Liventsev,[11] T. Matsumoto,[44] S. McOnie,[38] K. Miyabayashi,[21] H. Miyata,[27] Y. Miyazaki,[20] R. Mizuk,[11] D. Mohapatra,[46] G. R. Moloney,[19] Y. Nakahama,[42] E. Nakano,[29] M. Nakao,[8] Z. Natkaniec,[25] S. Nishida,[8] O. Nitoh,[45] S. Ogawa,[39] S. Okuno,[13] S. L. Olsen,[7] Y. Onuki,[33] H. Ozaki,[8] P. Pakhlov,[11] G. Pakhlova,[11] C. W. Park,[37] R. Pestotnik,[12] L. E. Piilonen,[46] Y. Sakai,[8] N. Satoyama,[36] T. Schietinger,[16] O. Schneider,[16] A. J. Schwartz,[3] R. Seidl,[9,33] K. Senyo,[20] M. E. Sevior,[19] M. Shapkin,[10] H. Shibuya,[39] J. B. Singh,[31] A. Somov,[3] N. Soni,[31] S. Stanič,[28] M. Starič,[12] H. Stoeck,[38] K. Sumisawa,[8] T. Sumiyoshi,[44] S. Suzuki,[34] F. Takasaki,[8] K. Tamai,[8] M. Tanaka,[8] G. N. Taylor,[19] Y. Teramoto,[29] X. C. Tian,[32] I. Tikhomirov,[11] T. Tsukamoto,[8] S. Uehara,[8] K. Ueno,[24] Y. Unno,[6] S. Uno,[8] Y. Ushiroda,[8] Y. Usov,[1] G. Varner,[7] K. E. Varvell,[38] S. Villa,[16] A. Vinokurova,[1] C. H. Wang,[23] Y. Watanabe,[43] E. Won,[14] B. D. Yabsley,[38] A. Yamaguchi,[41] Y. Yamashita,[26] M. Yamauchi,[8] Y. Yusa,[46] V. Zhilich,[1] V. Zhulanov,[1] and A. Zupanc[12]

(Belle Collaboration)

[1]*Budker Institute of Nuclear Physics, Novosibirsk*
[2]*Chiba University, Chiba*
[3]*University of Cincinnati, Cincinnati, Ohio 45221*
[4]*Department of Physics, Fu Jen Catholic University, Taipei*
[5]*The Graduate University for Advanced Studies, Hayama*
[6]*Hanyang University, Seoul*
[7]*University of Hawaii, Honolulu, Hawaii 96822*
[8]*High Energy Accelerator Research Organization (KEK), Tsukuba*
[9]*University of Illinois at Urbana-Champaign, Urbana, Illinois 61801*
[10]*Institute of High Energy Physics, Protvino*
[11]*Institute for Theoretical and Experimental Physics, Moscow*
[12]*J. Stefan Institute, Ljubljana*
[13]*Kanagawa University, Yokohama*
[14]*Korea University, Seoul*
[15]*Kyungpook National University, Taegu*
[16]*Swiss Federal Institute of Technology of Lausanne, EPFL, Lausanne*
[17]*University of Ljubljana, Ljubljana*
[18]*University of Maribor, Maribor*
[19]*University of Melbourne, School of Physics, Victoria 3010*
[20]*Nagoya University, Nagoya*
[21]*Nara Women's University, Nara*
[22]*National Central University, Chung-li*
[23]*National United University, Miao Li*
[24]*Department of Physics, National Taiwan University, Taipei*
[25]*H. Niewodniczanski Institute of Nuclear Physics, Krakow*
[26]*Nippon Dental University, Niigata*
[27]*Niigata University, Niigata*
[28]*University of Nova Gorica, Nova Gorica*
[29]*Osaka City University, Osaka*
[30]*Osaka University, Osaka*
[31]*Panjab University, Chandigarh*
[32]*Peking University, Beijing*

1550-7998/2007/76(9)/091103(7)

[33]RIKEN BNL Research Center, Upton, New York 11973
[34]Saga University, Saga
[35]Seoul National University, Seoul
[36]Shinshu University, Nagano
[37]Sungkyunkwan University, Suwon
[38]University of Sydney, Sydney, New South Wales
[39]Toho University, Funabashi
[40]Tohoku Gakuin University, Tagajo
[41]Tohoku University, Sendai
[42]Department of Physics, University of Tokyo, Tokyo
[43]Tokyo Institute of Technology, Tokyo
[44]Tokyo Metropolitan University, Tokyo
[45]Tokyo University of Agriculture and Technology, Tokyo
[46]Virginia Polytechnic Institute and State University, Blacksburg, Virginia 24061
[47]Yonsei University, Seoul

(Received 13 April 2007; published 27 November 2007)

We present measurements of time-dependent CP asymmetries in $B^0 \to \omega K_S^0$, $f_0(980)K_S^0$, $K_S^0\pi^0$ and $K^+K^-K_S^0$ decays based on a sample of 535×10^6 $B\bar{B}$ pairs collected at the $\Upsilon(4S)$ resonance with the Belle detector at the KEKB energy-asymmetric e^+e^- collider. One neutral B meson is fully reconstructed in one of the specified decay channels, and the flavor of the accompanying B meson is identified from its decay products. CP-violation parameters for each of the decay modes are obtained from the asymmetries in the distributions of the proper-time intervals between the two B decays.

DOI: 10.1103/PhysRevD.76.091103 PACS numbers: 11.30.Er, 12.15.Hh, 13.25.Hw

The standard model (SM) describes CP violation in B^0 meson decays as being due to a complex phase of the 3×3 Cabibbo-Kobayashi-Maskawa mixing matrix [1]. In the decay chain $\Upsilon(4S) \to B^0\bar{B}^0 \to f_{CP}f_{\rm tag}$, where one of the B mesons decays at time t_{CP} to a CP eigenstate f_{CP} and the other decays at time $t_{\rm tag}$ to a final state $f_{\rm tag}$ that distinguishes between B^0 and $\bar{B}^0$, the decay rate has a time dependence [2] given by

$$\mathcal{P}(\Delta t) = \frac{e^{-|\Delta t|/\tau_{B^0}}}{4\tau_{B^0}} \times \{1 + q \cdot [\mathcal{S}_f \sin(\Delta m_d \Delta t) + \mathcal{A}_f \cos(\Delta m_d \Delta t)]\}. \quad (1)$$

Here $\mathcal{S}_f$ and $\mathcal{A}_f$ are CP violation parameters, τ_{B^0} is the B^0 lifetime, Δm_d the mass difference between the two B^0 mass eigenstates, $\Delta t = t_{CP} - t_{\rm tag}$, and the b-flavor charge q equals $+1$ (-1) when the tagging B meson is a B^0 $(\bar{B}^0)$. For most decays that proceed via the transition $b \to s\bar{q}q$ $(q = u, d, s)$, the SM predicts $\mathcal{S}_f \simeq -\xi_f \sin 2\phi_1$ and $\mathcal{A}_f \simeq 0$, where $\xi_f = +1$ (-1) for CP-even (CP-odd) final states [3]. If there is physics beyond the SM, the amplitudes for these decays may receive significant contributions that depend on a new phase that is different from ϕ_1. A comparison of the effective $\sin 2\phi_1$ values, $\sin 2\phi_1^{\rm eff}$ observed in these decays, with $\sin 2\phi_1$ obtained from the decays governed by the $b \to c\bar{c}s$ transition is thus an important test of the SM.

Among the final states studied here, ωK_S^0 and $K_S^0\pi^0$ are CP-odd, $f_0(980)K_S^0$ is CP-even, while $K^+K^-K_S^0$ is a mixture of both $\xi_f = -1$ and $+1$. The SM expectation for the latter mode is $\mathcal{S}_f = -(2f_+ - 1)\sin 2\phi_1$, where f_+ is the CP-even fraction. Excluding K^+K^- pairs that are consistent with a $\phi \to K^+K^-$ decay from the $B^0 \to K^+K^-K_S^0$ sample, we find that the $K^+K^-K_S^0$ state is primarily $\xi_f = +1$; a measurement of f_+ was obtained using an isospin relation [4] with a 357 fb^{-1} data sample and gave $f_+ = 0.93 \pm 0.09(\mathrm{stat}) \pm 0.05(\mathrm{syst})$; this implies an effective $\xi_f = 0.86 \pm 0.18 \pm 0.09$.

Recently, it was found that the direct CP asymmetries in $B^0 \to K^+\pi^-$ and $B^+ \to K^+\pi^0$ differ significantly [5], contrary to expectations that they would be the same [6]. Additional insight into this situation may be provided by a comparison of the measured value for $\mathcal{A}_f(B^0 \to K_S\pi^0)$ with the value predicted by a sum rule [7] using asymmetry measurements from the other $B \to K\pi$ decays. Previous measurements of CP asymmetries in $b \to s\bar{q}q$ transitions have been reported by Belle [8,9] and *BABAR* [10]. Belle's previously published results for $B^0 \to \omega K_S^0$, $f_0(980)K_S^0$, $K_S^0\pi^0$ and $K^+K^-K_S^0$ were based on a 253 fb^{-1} data sample corresponding to 275×10^6 $B\bar{B}$ pairs. Here we report measurements incorporating an additional 239 fb^{-1} data sample for a total of 492 fb^{-1} (535×10^6 $B\bar{B}$ pairs), and improvements to the analysis method that increase its sensitivity.

At the KEKB energy-asymmetric e^+e^- (3.5 on 8.0 GeV) collider [11], the $\Upsilon(4S)$ is produced with a Lorentz boost of $\beta\gamma = 0.425$ nearly along the z axis, which is defined as opposite to the positron beam direction. Since the B^0 and $\bar{B}^0$ are approximately at rest in the $\Upsilon(4S)$ center-of-mass system (cms), Δt can be determined from the displacement in z between the two decay vertices: $\Delta t \simeq \Delta z/(\beta\gamma c)$.

The Belle detector is a large-solid-angle magnetic spectrometer that consists of a silicon vertex detector (SVD), a 50-layer central drift chamber (CDC), an array of aerogel threshold Čerenkov counters (ACC), a barrel-like arrangement of time-of-flight scintillation counters (TOF), and an electromagnetic calorimeter (ECL) comprised of CsI(Tl) crystals located inside a superconducting solenoid coil that provides a 1.5 T magnetic field. An iron flux return located outside the coil is instrumented to detect K_L^0 mesons and to identify muons. The detector is described in detail elsewhere [12]. Two different inner detector configurations were used. For the first sample of 152×10^6 $B\bar{B}$ pairs, a 2.0 cm radius beampipe and a 3-layer silicon vertex detector (SVD-I) were used; for the latter 383×10^6 $B\bar{B}$ pairs, a 1.5 cm radius beampipe, a 4-layer silicon detector (SVD-II), and a small-cell inner drift chamber were used [13].

The intermediate meson states are reconstructed from the following decays: $\pi^0 \to \gamma\gamma$, $K_S^0 \to \pi^+\pi^-$, $\omega \to \pi^+\pi^-\pi^0$ and $f_0(980) \to \pi^+\pi^-$. Charged tracks, except those from $K_S^0 \to \pi^+\pi^-$ decays, are required to originate from the interaction point (IP). We distinguish charged kaons from pions based on a kaon (pion) likelihood $\mathcal{L}_{K(\pi)}$ derived from the TOF, ACC, and dE/dx measurements in the CDC. Photons are identified as isolated ECL clusters that do not match to any charged track. To reconstruct the ω candidates, candidate photons from $\pi^0 \to \gamma\gamma$ decays are required to have $E_\gamma > 0.05$ GeV. The π^0 candidates must have invariant masses that satisfy $0.118\ \mathrm{GeV}/c^2 < M_{\gamma\gamma} < 0.150\ \mathrm{GeV}/c^2$ and have momentum in the cms greater than 0.35 GeV/c. The $\pi^+\pi^-\pi^0$ invariant mass is required to be within 0.03 GeV/c^2 of the nominal ω mass. Pairs of oppositely charged pions that have invariant masses between 0.890 and 1.088 GeV/c^2 are used to reconstruct $f_0(980) \to \pi^+\pi^-$ decays. For the $B^0 \to K_S^0\pi^0$ mode, candidate photons are required to have $E_\gamma > 0.05$ GeV (0.1 GeV) in the barrel (end caps) and the reconstructed π^0 candidate is required to satisfy $0.115\ \mathrm{GeV}/c^2 < M_{\gamma\gamma} < 0.152\ \mathrm{GeV}/c^2$. In the $K^+K^-K_S^0$ reconstruction, we exclude the candidates with K^+K^- pair within 15 MeV/c^2 of the nominal ϕ meson mass to reduce the ϕ contribution to a negligible level. The K_S^0 selection criteria are the same as those described in Ref. [8].

We identify B meson decays using the energy difference $\Delta E \equiv E_B^{\mathrm{cms}} - E_{\mathrm{beam}}^{\mathrm{cms}}$ and the beam-energy-constrained mass $M_{\mathrm{bc}} \equiv \sqrt{(E_{\mathrm{beam}}^{\mathrm{cms}})^2 - (p_B^{\mathrm{cms}})^2}$, where $E_{\mathrm{beam}}^{\mathrm{cms}}$ is the beam energy in the cms, and E_B^{cms} and p_B^{cms} are the cms energy and momentum, respectively, of the reconstructed B candidate. The signal candidates are selected by requiring $5.27\ \mathrm{GeV}/c^2 < M_{\mathrm{bc}} < 5.29\ \mathrm{GeV}/c^2$ and that ΔE be in a restricted range that depends on the decay mode: $(-0.10, 0.08)$ GeV for ωK_S^0, $(-0.06, 0.06)$ GeV for $f_0(980)K_S^0$, $(-0.15, 0.10)$ GeV for $K_S^0\pi^0$ and $(-0.04, 0.04)$ GeV for $K^+K^-K_S^0$ candidates. The dominant background for the $b \to s\bar{q}q$ signal comes from continuum events ($e^+e^- \to u\bar{u}, d\bar{d}, s\bar{s}, c\bar{c}$). We discriminate against these backgrounds using event topology: continuum events tend to be jetlike in the cms, while $e^+e^- \to B\bar{B}$ events tend to be spherical. To quantify event topology, we calculate modified Fox-Wolfram moments and combine them into a Fisher discriminant [8]. We calculate a probability density function (PDF) for this discriminant and multiply it by a PDF for $\cos\theta_B$, where θ_B is the angle in the cms between the B direction and the beam axis. The PDFs for signal and continuum are obtained from Monte Carlo (MC) simulation and a data sideband, respectively. These PDFs are then used to calculate a signal (background) likelihood $\mathcal{L}_{\mathrm{sig(bkg)}}$, and we impose mode-dependent requirements on the likelihood ratio $\mathcal{R}_{\mathrm{s/b}} \equiv \mathcal{L}_{\mathrm{sig}}/(\mathcal{L}_{\mathrm{sig}} + \mathcal{L}_{\mathrm{bkg}})$.

The b-flavor of the accompanying B meson is identified by a tagging algorithm [14] that categorizes charged leptons, kaons and Λ's found in the event. The algorithm returns two parameters: the b-flavor charge q and r, which indicates the tag quality as determined from MC simulation and varies from $r = 0$ for no flavor discrimination to $r = 1$ for unambiguous flavor assignment. If $r < 0.1$, the accompanying B meson provides negligible tagging information and we set the wrong tag fraction to 0.5. Events with $r > 0.1$ are sorted into six r intervals.

The vertex position for the f_{CP} decay is reconstructed using charged tracks that have enough SVD hits. A constraint on the IP is also used with the selected tracks; the IP profile is convolved with the finite B flight length in the plane perpendicular to the z axis. The pions from K_S^0 decays are not used for vertexing except in the analysis of $B^0 \to K_S^0\pi^0$. The typical vertex reconstruction efficiency and z resolution are 95% and 78 μm, except for $B^0 \to K_S^0\pi^0$ decays. The vertex for $B^0 \to K_S^0\pi^0$ decays is reconstructed using the K_S^0 trajectory and the IP constraint, where both pions from the K_S^0 are required to have enough SVD hits in the same way as that for other f_{CP} decays. The vertex reconstruction efficiency depends both on the K_S^0 momentum and on the SVD geometry; the efficiency with SVD-II (32%) is higher than that with SVD-I (23%) because of the larger outer radius and the additional layer. The typical z resolution of the vertex reconstructed with the K_S^0 is 93 μm for SVD-I and 110 μm for SVD-II. The f_{tag} vertex determination is obtained with well-reconstructed tracks that are not assigned to f_{CP}. The typical vertex reconstruction efficiency and z resolution are 93% and 140 μm.

Figure 1 shows the reconstructed variables M_{bc}, ΔE and $\mathcal{R}_{\mathrm{s/b}}$ after flavor tagging and vertex reconstruction (before vertex reconstruction for the decay $B^0 \to K_S^0\pi^0$). The signal yield for each mode is obtained from an unbinned maximum-likelihood fit to these distributions; the $M(\pi^+\pi^-\pi^0)$ distribution is also included in the fit for the $B^0 \to \omega K_S^0$ mode. The signal shape for each decay mode is determined from MC events; these shapes are

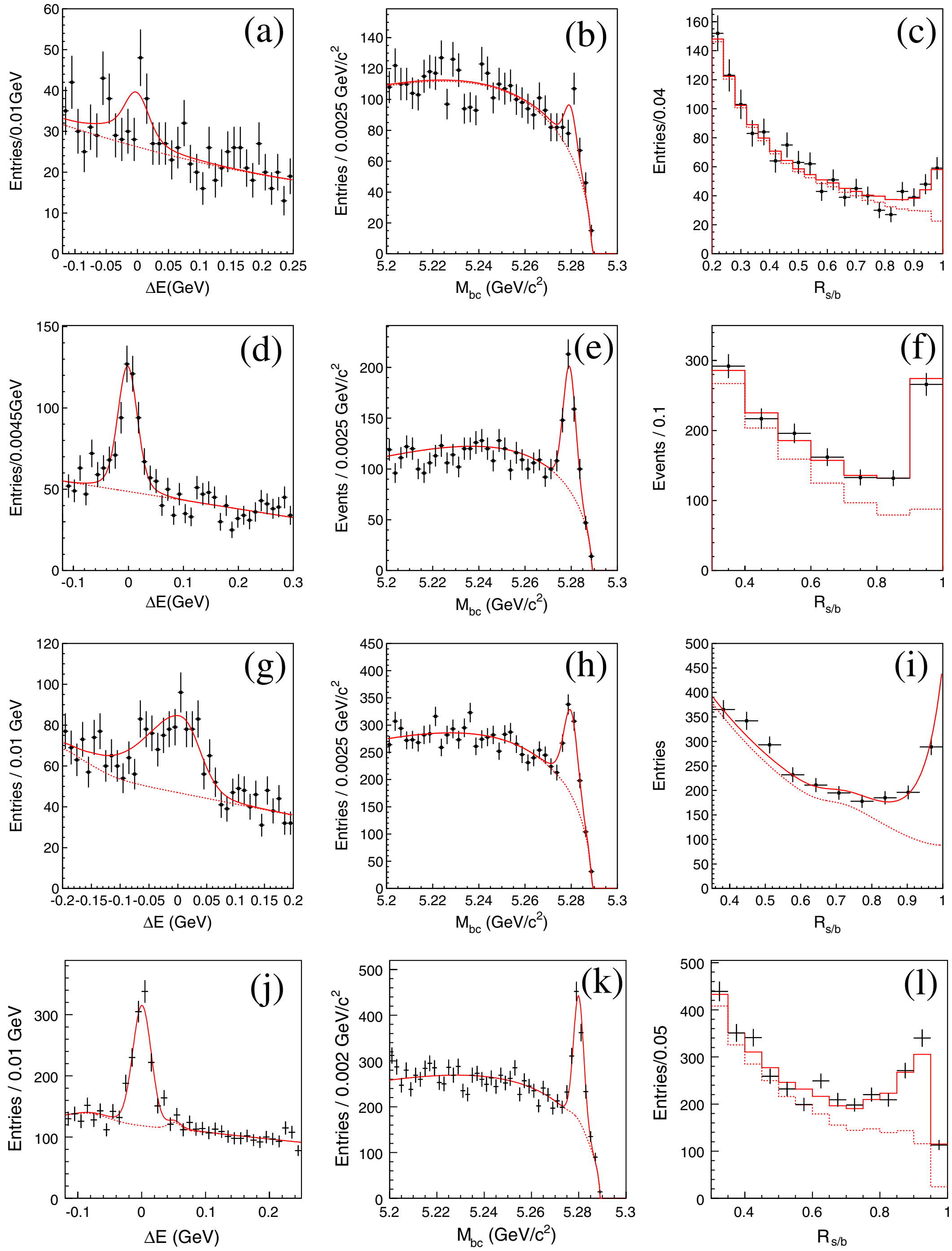

FIG. 1 (color online). ΔE distribution within the M_{bc} signal region and with $\mathcal{R}_{\mathrm{s/b}} > 0.5$, M_{bc} distribution within the ΔE signal region and with $\mathcal{R}_{\mathrm{s/b}} > 0.5$ and $\mathcal{R}_{\mathrm{s/b}}$ distribution within the $M_{\mathrm{bc}} - \Delta E$ signal region for (a), (b), (c) $B^0 \to \omega K_S^0$, (d), (e), (f) $B^0 \to f_0 K_S^0$, (g), (h), (i) $B^0 \to K_S^0 \pi^0$ and (j), (k), (l) $B^0 \to K^+ K^- K_S^0$. The solid curves show the fits to signal plus background distributions, and the dashed curves show the background contributions.

adjusted for small differences between MC and data using control samples that have similar final states but higher statistics [e.g. $B^- \to f_0(980)K^-$ to calibrate $B^0 \to f_0(980)K_S^0$]. The background has two components: continuum, which is modeled using events outside the signal region, and $B\bar{B}$ background, which is modeled with MC events. The signal yields in the ΔE-M_{bc} signal window are summarized in Table I.

In the signal distribution PDF [Eq. (1)], the effect of incorrect flavor assignment is incorporated and the result is convolved with a resolution function $R_{\mathrm{sig}}(\Delta t)$ to take into account the finite vertex resolution. The resolution function

TABLE I. Estimated signal yields $N_{\rm sig}$ in the signal region for each mode.

Mode	ξ_f	$N_{\rm sig}$
ωK_S^0	-1	118 ± 18
$f_0 K_S^0$	$+1$	377 ± 25
$K_S^0 \pi^0$	-1	515 ± 32
$K^+K^-K_S^0$	$+0.86 \pm 0.18 \pm 0.09$	840 ± 34

parameters, along with the wrong tag fractions for the six r intervals, w_l ($l = 1, 6$) and possible differences in w_l between B^0 and $\bar{B}^0$ decays (Δw_l) are determined using a high-statistics control sample of semileptonic and hadronic $b \to c$ decays [8,15].

We determine the following likelihood for each event:

$$P_i = (1 - f_{\rm ol}) \int [f_{\rm sig} \mathcal{P}_{\rm sig}(\Delta t') R_{\rm sig}(\Delta t_i - \Delta t') + (1 - f_{\rm sig}) \mathcal{P}_{\rm bkg}(\Delta t') R_{\rm bkg}(\Delta t_i - \Delta t')] d(\Delta t') + f_{\rm ol} P_{\rm ol}(\Delta t_i). \quad (2)$$

The signal probability $f_{\rm sig}$ depends on the r region and is calculated on an event-by-event basis as a function of $M_{\rm bc}$, ΔE and $\mathcal{R}_{\rm s/b}$ [and $M(\pi^+\pi^-\pi^0)$ for $B^0 \to \omega K_S^0$]. The addition of $\mathcal{R}_{\rm s/b}$ is one of the main improvements compared to our previous analysis [8].

For $B^0 \to f_0(980) K_S^0$, the fit to the ΔE, $M_{\rm bc}$ and $\mathcal{R}_{\rm s/b}$ distributions yields the number of $B^0 \to \pi^+\pi^- K_S^0$ candidates that have $\pi^+\pi^-$ invariant mass within the $f_0(980)$ resonance region, which includes other contributions (e.g. $B^0 \to \rho^0 K_S^0$, $K^*\pi^\pm$ and nonresonant three-body decays) which peak like the signal. To estimate these peaking backgrounds, we perform a fit to the $\pi^+\pi^-$ invariant mass distribution for the events inside the ΔE-$M_{\rm bc}$ signal region. We use Breit-Wigner functions for the ρ^0 and for a possible resonance above the $f_0(980)$ mass region, which is referred to as $f_X(1300)$ [16], with $M = 1.449\ {\rm GeV}/c^2$ and $\Gamma = 0.126\ {\rm GeV}/c^2$. A Flatté parametrization [17] is used for the $f_0(980)$ and an empirical model is used for the sum of the other components ($K^*(892)\pi$, $K_0^*(1430)\pi$ and nonresonant). The parameters of these PDFs and the model are fixed from data measurements [18]. The shape of the combinatorial background is obtained from a ΔE-$M_{\rm bc}$ sideband region. The $\pi^+\pi^-$ invariant mass distribution after background subtraction is shown in Fig. 2 along with the fit result. The fit yields 337 ± 27 $B^0 \to f_0(980) K_S^0$ events.

In Eq. (2), the PDF for background events, $\mathcal{P}_{\rm bkg}(\Delta t)$, is modeled as a sum of exponential and prompt components and is convolved with a sum of two Gaussians, $R_{\rm bkg}$. Parameters in $\mathcal{P}_{\rm bkg}(\Delta t)$ and $R_{\rm bkg}$ are determined from a fit to the Δt distribution for events in a ΔE-$M_{\rm bc}$ data sideband. $P_{\rm ol}(\Delta t)$ is a broad Gaussian function that represents an outlier component with a small fraction $f_{\rm ol}$. The only free parameters in the final fit are $\mathcal{S}_f$ and $\mathcal{A}_f$; these are determined by maximizing the likelihood function $L = \prod_i P_i(\Delta t_i; \mathcal{S}_f, \mathcal{A}_f)$ where the product is over all events.

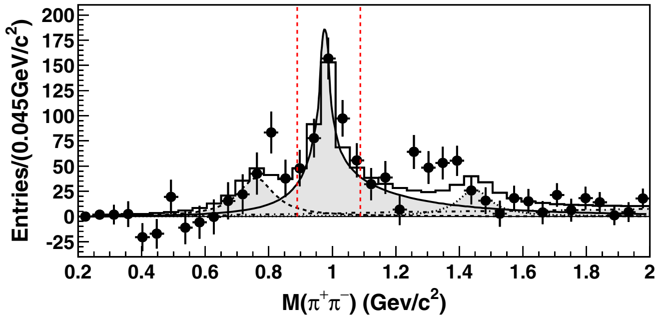

FIG. 2 (color online). $\pi^+\pi^-$ mass distribution for the $f_0 K_S^0$ events in the ΔE-$M_{\rm bc}$ signal box (shown here after background subtraction). The histogram is the result of the fit whereas the contributions are shown (solid line for $f_0(980)$, dashed for ρ^0 and dotted for $f_X(1300)$).

Table II summarizes the results of the fit for $\sin 2\phi_1^{\rm eff}$ and $\mathcal{A}_f$. For $B^0 \to K^+K^-K_S^0$, the SM prediction is given by $\mathcal{S}_f = -(2f_+ - 1)\sin 2\phi_1^{\rm eff}$. The effective $\sin 2\phi_1$ value for this mode is found to be $+0.68 \pm 0.15 \pm 0.03^{+0.21}_{-0.13}$. The third error is an additional systematic error arising from the uncertainty in f_+. We define the raw asymmetry in each Δt bin by $(N_+ - N_-)/(N_+ + N_-)$, where $N_{+(-)}$ is the number of observed candidates with $q = +1$ (-1). Figure 3 shows this asymmetry for events with good tag quality ($r > 0.5$) in each mode.

The dominant sources of systematic error for $\mathcal{S}_f$ are the uncertainties in the vertex reconstruction (0.01), in the background fraction (from 0.01 for $K_S\pi^0$ to 0.04 for ωK_S^0) and in the background Δt distribution (0.04 for $K_S\pi^0$ and 0.01 or less for others), and in the resolution function (0.05 for ωK_S and $K_S\pi^0$). The dominant sources of systematic error for $\mathcal{A}_f$ are the effects of tag-side interference [19] (0.04), the uncertainties in the vertex reconstruction (0.02), in the background fraction (0.03 for $f_0 K_S^0$ and ωK_S^0 and <0.02 for others). For the $f_0 K_S^0$ mode, additional systematics were included: uncertainties from the $M(\pi\pi)$ fit (0.06 for $\mathcal{S}_f$) and from the uncertainty in the CP content of the peaking background (0.08 for $\mathcal{S}_f$ and

TABLE II. Results of the fits to the Δt distributions. The first error is statistical and the second error is systematic. The third error for $\sin 2\phi_1^{\rm eff}$ of $K^+K^-K_S^0$ is an additional systematic error arising from the uncertainty in the $\xi_f = +1$ fraction.

Mode	$\sin 2\phi_1^{\rm eff}$	$\mathcal{A}_f$
ωK_S^0	$+0.11 \pm 0.46 \pm 0.07$	$-0.09 \pm 0.29 \pm 0.06$
$f_0 K_S^0$	$+0.18 \pm 0.23 \pm 0.11$	$-0.15 \pm 0.15 \pm 0.07$
$K_S^0 \pi^0$	$+0.33 \pm 0.35 \pm 0.08$	$-0.05 \pm 0.14 \pm 0.05$
$K^+K^-K_S^0$	$+0.68 \pm 0.15 \pm 0.03^{+0.21}_{-0.13}$	$-0.09 \pm 0.10 \pm 0.05$

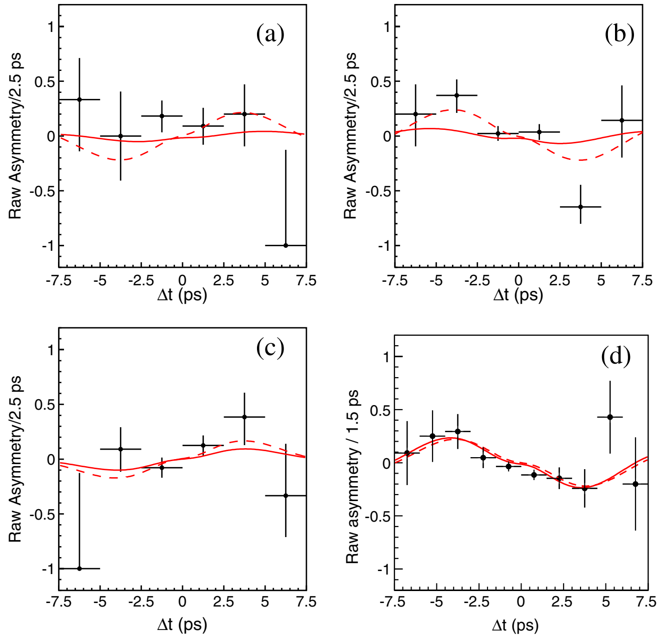

FIG. 3 (color online). Asymmetries of well-tagged events ($r > 0.5$) for (a) $B^0 \to \omega K_S^0$, (b) $B^0 \to f_0(980)K_S^0$, (c) $B^0 \to K_S^0\pi^0$ and (d) $B^0 \to K^+K^-K_S^0$. The solid curves show the results of the unbinned maximum-likelihood fits. The dashed curves show the SM expectation for the values of CP violation parameters obtained from $B^0 \to J/\psi K^0$ ($\sin 2\phi_1 = +0.642$ and $\mathcal{A}_f = 0$) [5].

0.04 for $\mathcal{A}_f$). For the $K_S^0\pi^0$ mode, the uncertainty in the rare B component is a significant contribution (0.04 for $\mathcal{S}_f$ and 0.02 for $\mathcal{A}_f$). Other contributions come from uncertainties in wrong tag fractions, lifetime and mixing. A possible fit bias is examined by fitting a large number of MC events. We add each contribution above in quadrature to obtain the total systematic uncertainty.

In summary, we have performed improved measurements of CP-violation parameters $\sin 2\phi_1^{\rm eff}$ and $\mathcal{A}_f$ for $B^0 \to \omega K_S^0$, $f_0(980)K_S^0$, $K_S^0\pi^0$ and $K^+K^-K_S^0$ using 535×10^6 $B\bar{B}$ events. These measurements supersede our previous results. Comparing the results for each individual $b \to s$ mode with those from measurements of $B^0 \to J/\psi K^0$ [5], we do not find any deviations that are in excess of two standard deviations.

We thank the KEKB group for the excellent operation of the accelerator, the KEK cryogenics group for the efficient operation of the solenoid, and the KEK computer group and the National Institute of Informatics for valuable computing and Super-SINET network support. We acknowledge support from the Ministry of Education, Culture, Sports, Science, and Technology of Japan and the Japan Society for the Promotion of Science; the Australian Research Council and the Australian Department of Education, Science and Training; the National Science Foundation of China and the Knowledge Innovation Program of the Chinese Academy of Sciences under Contracts No. 10575109 and IHEP-U-503; the Department of Science and Technology of India; the BK21 program of the Ministry of Education of Korea, the CHEP SRC program and Basic Research program (Grant No. R01-2005-000-10089-0) of the Korea Science and Engineering Foundation, and the Pure Basic Research Group program of the Korea Research Foundation; the Polish State Committee for Scientific Research; the Ministry of Education and Science of the Russian Federation and the Russian Federal Agency for Atomic Energy; the Slovenian Research Agency; the Swiss National Science Foundation; the National Science Council and the Ministry of Education of Taiwan; and the U.S. Department of Energy.

[1] N. Cabbibo, Phys. Rev. Lett. **10**, 531 (1963); M. Kobayashi and T. Maskawa, Prog. Theor. Phys. **49**, 652 (1973).
[2] A. B. Carter and A. I. Sanda, Phys. Rev. D **23**, 1567 (1981); I. I. Bigi and A. I. Sanda, Nucl. Phys. **B193**, 85 (1981).
[3] Y. Grossman and M. P. Worah, Phys. Lett. B **395**, 241 (1997); R. Fleischer, Int. J. Mod. Phys. A **12**, 2459 (1997); M. Ciuchini, E. Franco, G. Martinelli, A. Masiero, and L. Silvestrini, Phys. Rev. Lett. **79**, 978 (1997); D. London and A. Soni, Phys. Lett. B **407**, 61 (1997).
[4] A. Garmash *et al.* (Belle Collaboration), Phys. Rev. D **69**, 012001 (2004).
[5] E. Barberio *et al.* (Heavy Flavour Averaging Group), arXiv:hep-ex/0603003. See http://www.slac.stanford.edu/xorg/hfag/ for updated results.
[6] M. Gronau and J. L. Rosner, Phys. Rev. D **59**, 113002 (1999).
[7] D. Atwood and A. Soni, Phys. Rev. D **58**, 036005 (1998); M. Gronau, Phys. Lett. B **627**, 82 (2005).
[8] K-F. Chen *et al.* (Belle Collaboration), Phys. Rev. D **72**, 012004 (2005).
[9] K-F. Chen *et al.* (Belle Collaboration), Phys. Rev. Lett. **98**, 031802 (2007).
[10] B. Aubert *et al.* (*BABAR* Collaboration) Phys. Rev. D **71**, 091102 (2005); **71**, 111102 (2005); **74**, 011106 (2006); Phys. Rev. Lett. **98**, 051803 (2007); **98**, 031801 (2007); Phys. Rev. D **76**, 071101(R) (2007).
[11] S. Kurokawa and E. Kikutani, Nucl. Instrum. Methods Phys. Res., Sect. A **499**, 1 (2003), and other papers included in this volume.
[12] A. Abashian *et al.* (Belle Collaboration), Nucl. Instrum.

Methods Phys. Res., Sect. A **479**, 117 (2002).

[13] Z. Natkaniec (Belle SVD2 Group), Nucl. Instrum. Methods Phys. Res., Sect. A **560**, 1 (2006).

[14] H. Kakuno *et al.*, Nucl. Instrum. Methods Phys. Res., Sect. A **533**, 516 (2004).

[15] K. Abe *et al.* (Belle Collaboration), Phys. Rev. D **71**, 072003 (2005).

[16] A. Garmash *et al.* (Belle Collaboration), Phys. Rev. Lett. **96**, 251803 (2006).

[17] S. M. Flatté, Phys. Lett. **63B**, 224 (1976).

[18] A. Garmash *et al.* (Belle Collaboration), Phys. Rev. D **75**, 012006 (2007).

[19] O. Long, M. Baak, R. N. Cahn, and D. Kirkby, Phys. Rev. D **68**, 034010 (2003).